



Thorium-232 fission induced by light charged particles up to 70 MeV

Vincent Métivier, Charlotte Duchemin, Arnaud Guertin, N. Michel, Ferid
Haddad

► **To cite this version:**

Vincent Métivier, Charlotte Duchemin, Arnaud Guertin, N. Michel, Ferid Haddad. Thorium-232 fission induced by light charged particles up to 70 MeV. EPJ Web of Conferences, EDP Sciences, 2017, 146, pp.04058. 10.1051/epjconf/201714604058 . in2p3-01951317

HAL Id: in2p3-01951317

<http://hal.in2p3.fr/in2p3-01951317>

Submitted on 11 Dec 2018

HAL is a multi-disciplinary open access archive for the deposit and dissemination of scientific research documents, whether they are published or not. The documents may come from teaching and research institutions in France or abroad, or from public or private research centers.

L'archive ouverte pluridisciplinaire **HAL**, est destinée au dépôt et à la diffusion de documents scientifiques de niveau recherche, publiés ou non, émanant des établissements d'enseignement et de recherche français ou étrangers, des laboratoires publics ou privés.

Thorium-232 fission induced by light charged particles up to 70 MeV

Vincent Métivier^{1,a}, Charlotte Duchemin¹, Arnaud Guertin¹, Nathalie Michel², and Férid Haddad^{1,2}

¹ Laboratoire Subatech, IN2P3-CNRS, Ecole des Mines de Nantes, Université de Nantes, 4 rue Alfred Kastler, 44307 Nantes, France

² GIP ARRONAX, 1 rue Aronnax, 44817 Saint Herblain, France

Abstract. Studies have been devoted to the production of alpha emitters for medical application in collaboration with the GIP ARRONAX that possesses a high energy and high intensity multi-particle cyclotron. The productions of Ra-223, Ac-225 and U-230 have been investigated from the Th-232(p,x) and Th-232(d,x) reactions using the stacked-foils method and gamma spectrometry measurements. These reactions have led to the production of several fission products, including some with a medical interest like Mo-99, Cd-115g and I-131. This article presents cross section data of fission products obtained from these undedicated experiments. These data have been also compared with the TALYS code results.

1. Introduction

The irradiation of thorium by light charged particles like protons and deuterons leads to the production of several radionuclides among which radium-223 [1], bismuth-213 [2] and thorium-226 [3], alpha emitters having a great potential in oncologic therapy. The GIP ARRONAX is focused on the production of medically relevant radionuclides and possesses a multi-particle cyclotron [4]. This accelerator has been used for our study on the Th-232(p,x) and Th-232(d,x) reactions. The main motivation was to study the production cross section of Pa-230 that decays to Th-226 [5] via U-230. After the irradiations, the activity values were determined by gamma spectrometry, and the associated spectra give information on the production of several fission products inside the thorium-232 target. The activity of each detectable and quantifiable fission product (FP) has been determined and their associated production cross section has been extracted. From these data, we determined the mass distribution of the FP and the sum of the fission product cross section values. A systematic comparison with the results of the TALYS code has been done.

2. Material and methods

2.1. Experimental set-up

The cross section data are obtained using the stacked-foils method [5,6], which consists of the irradiation of a set of thin foils, grouped as patterns. Each pattern contains a target to produce the isotopes of interest. Each target is followed by a monitor foil to have information on the beam intensity thanks to the use of a reference reaction recommended by the International Atomic Energy Agency [7]. In our experiment, the monitor foil acts also as a catcher to stop the recoil nuclei produced in the target foil. A degrader foil is placed after each monitor foil to

change the incident beam energy from one target foil to the next one. Each foil in the stack has been weighed before irradiation using an accurate scale ($\pm 10^{-5}$ g) and scanned to precisely determine its area. The thickness is deduced from these measurements, assuming that it is homogeneous over the whole surface. In this work, we used 10 and 40 μm thick thorium foils, 10 to 25 μm thick titanium, copper and nickel monitor foils depending on the incident particle and its energy, and 100 to 1000 μm thick aluminium or copper degrader foils. These foils were irradiated by the proton (up to 70 MeV) and deuteron (up to 33 MeV) beams provided by the ARRONAX cyclotron. Proton and deuteron beams have, respectively, an energy uncertainty of ± 0.50 MeV and ± 0.25 MeV, as specified by the cyclotron provider using simulations.

The beam line is under vacuum and closed using a 75 μm thick kapton foil. The stacks were located about 6.8 cm downstream in air. The energy through each target and monitor foils has been determined in the middle of the thickness of the foil using the SRIM software [8]. Energy losses in the kapton foil and air have been taken into account. Five stacks were irradiated with protons and five with deuterons, covering respectively, the energy range from 70 MeV down to 11 MeV and from 33 MeV down to 8 MeV. The use of several stacks allows us to minimize the energy uncertainty in our experiments. All along the stack, depending on the number of foils, the energy uncertainty increases up to ± 1.8 MeV due to the energy straggling. Irradiations were carried out for half an hour, with a mean intensity between 100 and 150 nA particles for proton beams and between 50 and 140 nA for deuteron beams. The recommended cross section values [7] of the Ti-nat(d,x)V-48 (all energies), Cu-nat(p,x)Co-56,Zn-62 (> 50 MeV), Ti-nat(p,x)V-48 (< 20 MeV) and Ni-nat(p,x)Ni-57 (20–50 MeV) reactions were used to get information on the beam intensity.

The activity measurements in each foil were performed using a high purity germanium detector with

^a e-mail: Vincent.Metivier@subatech.in2p3.fr

low-background lead and copper shielding. Gamma spectra were recorded in a suitable geometry calibrated in energy and efficiency with standard Co-57, Co-60 and Eu-152 gamma sources. The full widths at half maxima were 1.04 keV at 122 keV (Co-57 γ ray) and 1.97 keV at 1332 keV (Co-60 γ ray). The samples were placed at a distance of 19 cm from the detector which is suitable to reduce the dead time and the effect of sum peaks. The dead time during the counting was always kept below 10%. The first measurements started the day after the irradiation (after a minimum of 15 hours cooling time) during one hour, for all target and monitor/catcher foils. A second series of measurements was performed one week after the end of irradiation, during a minimum of 24 hours (one day) and up to 60 hours. A third series of measurements was done for long half-life radionuclides and waiting for the decay of some radionuclides. Our data are then limited to γ emitter radionuclides with a half-life higher than few hours. FP have been detected and quantified from Zn-72 to Pm-151. The majority of them have been measured after the decay of their parents (filiation).

2.2. Cross section calculation

The cross section values are calculated using the well-known activation formula, defined as a relative equation in which the knowledge of the beam current is no longer necessary thanks to the recommended reactions. The uncertainty is expressed as a propagation error calculation (see [9] for more details).

2.3. Catcher correction

In our experiments devoted to medical isotope production studies, only one catcher was placed and was necessary to collect the recoil nuclei after the target. However, in the case of fission, the FP are emitted both forward and backward direction from the target. The use of a catcher before the target should then be mandatory to collect all the nuclei. In order to correct it, the proportion of FP emitted backward the target has been estimated by kinematic and Monte Carlo calculations.

In our calculation, the projectile is sent on a thorium target followed by a catcher. The FP emission is computed in the centre of mass of the compound nucleus (Th+p or Th+d): the total kinetic energy is calculated according to the Viola et al. formula [10], both fragments are supposed to be emitted with an energy distributed according to the linear momentum conservation and distributed isotropically in the centre of mass of the reaction. The FP energy is then calculated in the laboratory system and its emission point randomly computed in the depth of the thorium target. Thanks to SRIM calculation [8], one can then determine if the FP remains in the target or exits it, forward or backward. Experimentally we know that FP from Zn-72 to Pm-151 have been detected. The proportion of FP in the target as well as backward and forward the target is determined in the case of Zn-72, I-131 and Pm-151. Fig. reffig1 shows these proportions as a function of the incident energy for proton beams.

Based on the results shown on Fig. 1, one can consider that approximatively the same amount of FP is collected in both catchers. This has been validated with a dedicated experiment with two catchers, forward and backward (see

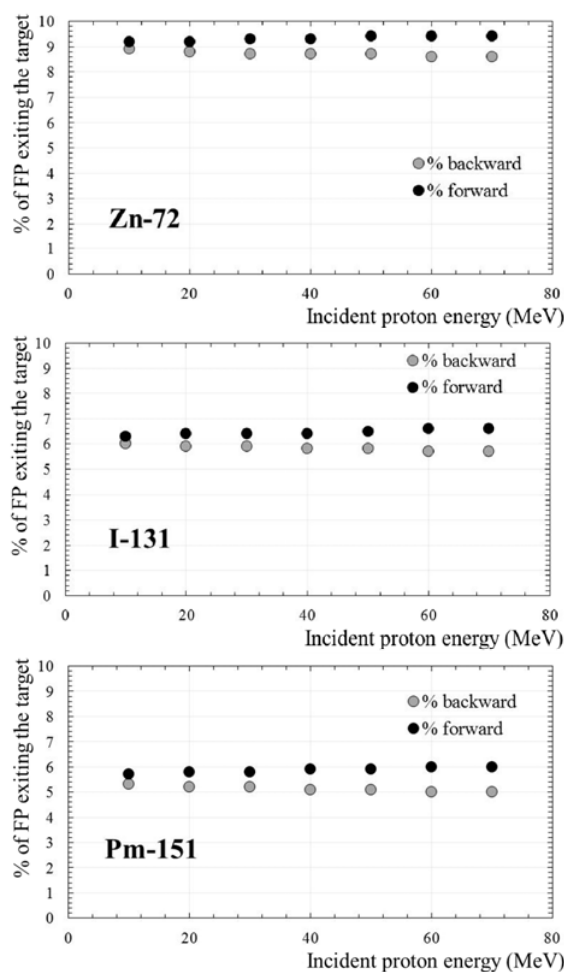


Figure 1. Fraction of fission products exiting the thorium target (40 μm thick), backward and forward, as a function of the incident proton energy.

Fig. 4). Thus, the amount of FP activity measured in the (forward) catcher is simply multiplied by a factor 2 and added to the activity obtained in the target to determine the cross section values discussed hereafter. The small difference due to kinematics between forward and backward visible on Fig. 1 is neglected compared to the uncertainty on the experimental determination of the activity on the catcher.

2.4. The TALYS code

In this work, all the experimental cross section values are compared with the version 1.6 of the TALYS code released in December, 2013 [11]. TALYS is a nuclear reaction program which simulates reactions induced by light particles on target nuclei heavier than carbon. It incorporates theoretical models to predict observables including cross section values as a function of the incident particle energy (from 1 keV to 1 GeV). A combination of models that best describes the whole set of available data for all projectiles, targets and incident energies have been defined by the authors and put as default in the code. In this way, a calculation can be performed with minimum information in the input file: the type of projectile and its incident energy, the target type and its mass.

Since there are some differences between experimental data and the results of the TALYS code using default

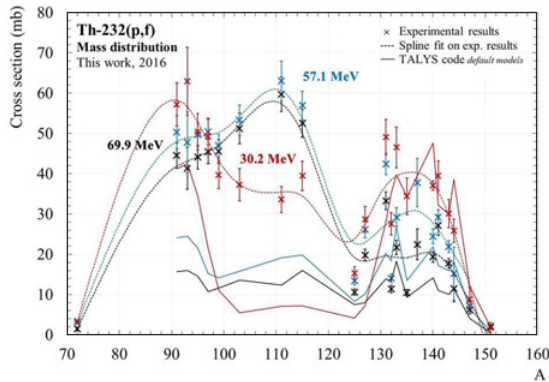


Figure 2. Mass distribution of the fission products for protons as projectiles.

models, we have defined a new combination of models, already included in the TALYS code. The description of the optical, preequilibrium and level density models have been found to have a great influence on the calculated production cross section values. Better results are, in general, obtained when proton and deuterons are used as projectile using the optical model described, respectively by [12] and [13]. And for both projectiles, but also with alpha particles [9], when a preequilibrium model based on the exciton model including numerical transition rates with optical model for collision probabilities [14] and a model for the microscopic level density from Hilaire's combinatorial tables [15] is used. The results referenced as TALYS 1.6 *Adj* in Figs. 4 and 5 correspond to TALYS calculations performed with this new combination of models.

3. Results and discussion

3.1. The mass distributions

The data depicted in Fig. 2 and Fig. 3 show the cumulative cross section values of the detected FP, respectively with protons and deuterons as projectiles, plotted as a function of the FP mass, A. The points correspond to our measurements and the dash lines are spline fits on these experimental values. The full lines to TALYS results with default models, selecting only FP that have been detected in our experimental conditions (presented at the end of the part 2.1). The apparent depletion of the heavier FP peak is due to these experimental conditions (γ spectrometry detectability).

Proton results (Fig. 2) show that the symmetric fission (highlighted around $A = 110$) becomes more probable than the asymmetric fission with the increase of the incident energy (above 30 MeV). This has already been observed with protons [16] and neutrons [17]. Figure 2 shows saturation, even decrease of the amplitude of the symmetric fission above 57 MeV. This trend has to be confirmed and explained. The cross section values are similar in the case of proton and deuteron irradiations (see Fig. 3) considering the same incident beam energy. In all cases, the TALYS code with default models is not able to reproduce our experimental data leading to a too low production of fission fragments.

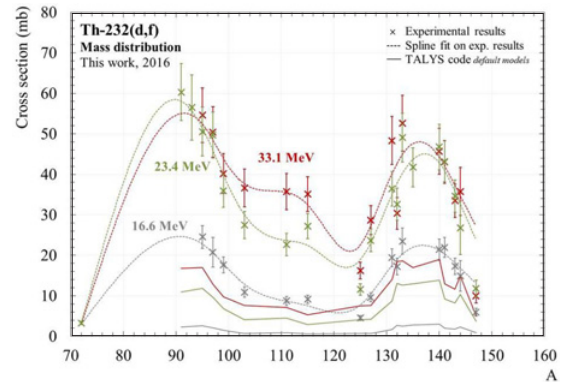


Figure 3. Mass distribution of the fission products for deuterons as projectiles.

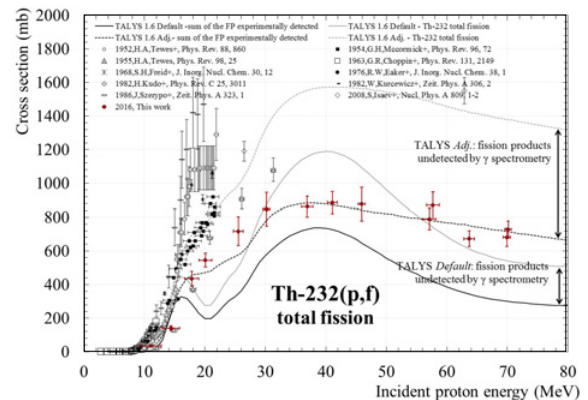


Figure 4. Th-232 total fission cross section for protons as projectiles.

3.2. The Th-232 total fission cross sections

Figure 4 and Fig. 5 show the sum of the FP production cross sections measured in our experiments, for protons and deuterons as projectiles, respectively. These plots also show the TALYS code results (limited to the detected FP) and the TALYS Th-232 total fission cross section (including all FP). For both projectiles, protons (Fig. 4) and deuterons (Fig. 5), our experimental total fission value reaches 800 mb for the incident energy of 30 MeV. Both curves show the same trend.

Figure 4 presents also the results from an experiment made with two catchers; one backward and one forward the target. Two energy points (69.9 MeV and 57.1 MeV) are in agreement with values obtained when only one catcher is placed forward relative to the beam direction and its contribution is doubled. This confirms our approach for the catcher correction.

In Fig. 4 and Fig. 5 TALYS results using the default models are referred as '*Default*' whereas those obtained using the combination of models described in the part 2.4 are referred as '*Adj.*'. We found that TALYS *Adj.* is more able to reproduce the shape and the amplitude of the FP cross sections than TALYS with default models. In addition, the TALYS *Adj.* results allow estimating the proportion of FP that have been produced during the irradiations but not detected in our experimental conditions (i.e. cooling time, γ spectrometry) by just subtracting the TALYS result without and with our experimental constrains.

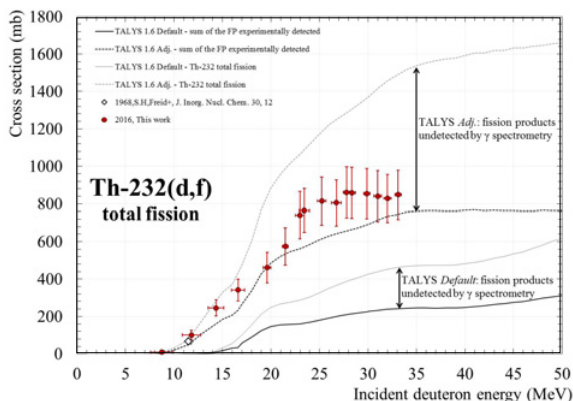


Figure 5. Th-232 total fission cross section for deuterons as projectiles.

4. Conclusion

Th-232(p,x) and Th-232(d,x) reactions have been studied using the stacked-foils method. These reactions have led to the production of several fission products. The absence of catcher backward the targets in our stacked-foils experiments has been corrected after kinematic and Monte Carlo calculations. These corrections have been validated by a dedicated experiment using two catchers.

Even if our work come from undedicated experiments and give partial measurements, the increase of symmetric fission of Th-232 with the proton and deuteron incident energy has been observed. Total fission cross sections have then been estimated thanks to TALYS calculations. A special effort has been done on the determination of which models included in the TALYS code can better reproduce the experimental data than the default ones, considering our experimental conditions. Our new experimental results could help to contribute to the improvement of the theoretical models. Studies are still in progress on this part.

The ARRONAX cyclotron is a project promoted by the Regional Council of Pays de la Loire financed by local authorities, the French government and the European Union. This work has been, in part, supported by a grant from the French National Agency for Research called “Investissements d’Avenir”, Equipex Arronax-Plus No. ANR-11-EQPX-0004 and Labex No. ANR- 11-LABX-0018-01.

References

- [1] M.R. Harrison, T.Z. Wong, A.J. Armstrong, D.J. George, *Manag. Res.* **5** (2013)
- [2] A. Morgenstern, et al., *Curr. Radiopharmaceutics* **5**, 221–7 (2012)
- [3] C. Friesen, et al., *Haematologica* **94**, 32 (2009)
- [4] F. Haddad, et al., *Eur. J. Nucl. Med. Mol. Imaging* **35**, 1377–87 (2008)
- [5] C. Duchemin, et al., *Phys. Med. Biol.* **60**, 931–46 (2015)
- [6] G. Blessing, et al., *Appl. Radiat. Isot.* **955**, 46–9 (1995)
- [7] F. Tárkányi, et al., *IAEA-TECDOC* **1211**, 49–152 (2001). Database available on <https://www-nds.iaea.org/medportal/>, update may 2013
- [8] J.F. Ziegler, et al., *Nucl. Instrum. Methods Phys. Res. B* **268**, 1818–23 (2010)
- [9] C. Duchemin, et al., *Appl. Radiat. Isot.* **115**, 113–124 (2016)
- [10] V.E. Viola, et al., K. Kwiatkowski, M. Walker, *Phys. Review C* **31**, 4 (1985)
- [11] A.J. Koning, D. Rochman, *Nucl. Data Sheets* **113**, 2841 (2012)
- [12] A.J. Koning, J.P. Delaroche, *Nucl. Phys. A* **707** (2002)
- [13] Y. Han, Y. Shi, Q. Shen, *Phys. Review C* **73** (2006)
- [14] E. Gadioli, P.E. Hodgson, Oxford Univ. Press (1992)
- [15] S. Goriely, S. Hilaire, A.J. Koning, *Phys. Review C* **78** (2008)
- [16] S I. Mulgin et al., *Nucl. Phys. A* **824** (2009) 1
- [17] I.V. Ryzhov et al., *Phys. Rev. C* **83**, 054603 (2011)